A radio continuum study of four spiral galaxies with an unusual radio morphology

Bruyn, A.G. de

Astron. Astrophys. 58, 221—236 (1977)

ASTRONOMY AND ASTROPHYSICS

A Radio Continuum Study of Four Spiral Galaxies with an Unusual Radio Morphology

A. G. de Bruyn*
Sterrewacht Leiden

Received October 1, revised November 15, 1976

Summary. High-resolution multi-frequency radio continuum data are presented of four spiral galaxies observed with the Westerbork Synthesis Radio Telescope. Among a large sample of spiral galaxies observed at Westerbork these four stand out because of their high surface brightness and lack of correlation between radio and optical structures.

NGC 4631, observed at 6 cm, contains a complex elongated radio structure in its central region with a linear dimension of about 2.5 kpc. Its surface brightness is about two orders of magnitude higher than that of the surrounding disk emission.

NGC 4258 was observed at 6 and 49 cm. The two anomalous radio spiral arms, detected previously at 21 cm, are found to terminate abruptly at the edge of the optical and HI disk providing strong evidence that they are in the plane of the galaxy.

NGC 2146, observed at wavelengths of 6 and 21 cm, has radio structure dominated by a narrow ridge of emission symmetrically extending to several kpc from the nucleus. Allowing for inclination effects, this ridge appears to be highly collimated in the azimuthal direction in the galaxy equatorial plane. Surrounding the ridge is an approximately circular plateau of much lower surface brightness.

NGC 3079, observed at 6 and 21 cm, has a peculiar radio structure in the form of a cross centered on the bright radio nucleus. One pair of arms of this cross is parallel to the galaxy major axis while the other pair is almost parallel to the minor axis of this highly inclined galaxy. Faint disk emission and protrusions from the plane have also been detected.

Upper limits are given to the linear polarization of these radio structures in the range of 0.5–15%. The available radio flux density measurements of NGC 2146 and NGC 3079 are used to construct accurate integrated spectra which are described by power laws with indices of -0.62 and -0.73, respectively. The anomalous radio structures in NGC 4631 and NGC 4258 have a spectral index of -0.6.

The origin of the radio structures in the galaxies is discussed using their radio spectra as basis. It is shown that the relativistic electrons giving rise to the radio emission must have been produced recently and it is suggested that high-speed gas expulsion from the nucleus has taken place in at least three of these galaxies. A similar suggestion has been made previously for the case of NGC 4258. Evidence exists for nuclear activity in the optical structures of these galaxies.

The frequency of nuclear activity in spirals leading to bright large scale anomalous radio structures is estimated and found to be comparable to the frequency of Seyfert activity in spiral galaxies. The differences in radio structures between spiral and elliptical galaxies are briefly discussed. The action of the interstellar medium in spiral galaxies may be crucial to the formation of bright anomalous radio structures.

Key words: spiral galaxy — radio structure — nuclear activity

1. Introduction

Our knowledge of the intensity and distribution of the radio continuum emission in spiral galaxies has undergone a remarkable increase in the past few years as a result of aperture synthesis studies of several tens of galaxies. A recent review of these observations is given by van der Kruit and Allen (1976). From these studies it is clear that the radio morphology of spiral galaxies covers a wide range in central concentration, disk and halo structure and prominence of spiral arms. In most spiral galaxies the observed radio structures still correlate reasonably well with major optical features (as, for example, in M 31, M 51 and M 101) but in some galaxies there is no obvious relationship between the two (e.g. NGC 4258). Although we are still far from a complete

* Now at Hale Observatories, 813 Santa Barbara Street, Pasadena, CA 91101, USA

Table 1. Observations and instrumental parameters

Galaxy		NGC 4631	NGC 4258		NGC 2146		NGC 3079	
Frequency/wavelength	[MHz/cm]	4995/6.0	4995/6.0	610/49.2	4995/6.0	1410/21.3[a]	4995/6.0	1410/21.3[a]
Observing dates		25 Feb. 1973	29 Oct. 1972	30 Sept. 1973	24 March 1974	20 July 1974	29 Dec. 1974	24 June 1975
		9 June 1973	4 Dec. 1972	19 Oct. 1973 4 Nov. 1973	23 May 1974		13 and 14 Jan. 1975	1 and 17 July 1975
Field centre (1950.0)		$12^h39^m40^s$ $+32°48'00''$	$12^h16^m26^s$ $+47°35'00''$	$12^h16^m30^s$ $+47°38'00''$	$06^h10^m45^s$ $+78°21'29''$	$06^h10^m45^s$ $+78°21'29''$	$09^h58^m33^s$ $+55°54'45''$	$09^h58^m33^s$ $+55°54'45''$
Total observing time	[h]	2 × 12	2 × 12	2 × 12	1 × 12	1 × 12	2 × 12	2 × 12
Baseline coverage[b]	[m]	36(36)1440	36(36)1440	36(36)1440	36(72)1404[c]	72(72)1440	36(36)1440	36(36)1440
Standard synthesized beam (half-power width RA × Dec)	["]	6.9 × 12.7	6.9 × 9.3	56 × 76	6.9 × 7.1	24 × 25	6.9 × 8.3	24 × 29
Flux density to brightness temperature conversion[d]	[K/mJy]	0.65	0.9	0.9	1.2	1.2	1.0	1.0
Grating ring separation (RA × Dec)	[']	5.7 × 10.5	5.7 × 7.8	47 × 64	2.9 × 2.9	10.2 × 10.4	5.7 × 6.9	20.3 × 24.6

[a] 21 cm line emission falls outside the receiver bandpass
[b] To read as: shortest baseline (increment) longest baseline
[c] Due to instrumental failure the data on baselines 36 and 108 m were not usable over a large part of the observed h angle range
[d] For extended structure in standard maps; in convolved maps the conversion factor decreases approximately inversely proportional to the beam area

understanding of the former, the context in which to search for the origin of the radio emission seems much better defined there than in the latter. In this paper we attempt to improve our knowledge of the anomalous radio structures in some spiral galaxies.

Radio continuum observations are presented here of four spiral galaxies with such anomalous structures. NGC 4631 and NGC 4258 have been mapped previously by Pooley (1969), van der Kruit (1973a) and van der Kruit et al. (1972). The initiative to observe NGC 2146 and NGC 3079 rests mainly on the fact that their radio emission is very intense and is confined to a region much less than the optical dimensions (Heeschen and Wade, 1964; Lequeux, 1971).

2. Observations and Reductions

All observations were made using the Westerbork Synthesis Radio Telescope (WSRT). Observations were obtained at frequencies of 610, 1410 and 4995 MHz; henceforth we will use the abbreviated wavelength notation 49, 21 and 6 cm. The telescope and its principles of operation have been described by Baars and Hooghoudt (1974) and Högbom and Brouw (1974). A description of the receiver can be found in Casse and Muller (1974). Standard calibration and reduction procedures were used as given in van Someren-Gréve (1974). The methods of polarization measurement have been described by Weiler (1973). At all three frequencies the system bandpass has a width of 4.2 MHz. During the period that the observations were made the system temperatures were 350 K (at 49 cm), 90 K (at 21 cm) and 240 K (at 6 cm). A summary of other relevant telescope and observational parameters is collected in Table 1.

Before Fourier transformation of the data they were weighted with a Gaussian function that reaches a value of 0.25 at the longest baseline in use in the observations (L_{max}). This yields a synthesized beam with half-power width of $0.80\,\lambda/L_{max}$ radians in right ascension and a factor $\mathrm{cosec}\,\delta$ larger in declination. For this beam shape, and structure in the range of spatial frequencies observed, the conversion of peak flux density S (in mJy[1]) to brightness temperature T (in K) is given to within 5% by $T = 1.21\,S\sin\delta$. Typical synthesized fields of view measured 3.4° (at 49 cm), 1.5° (at 21 cm) and 0.35° (at 6 cm) while the primary beam widths at half-power are 82′, 37′ and 11′. The effects of background sources in the maps were removed when necessary. There is no apparent connection between any of these background sources and the galaxy under investigation. In some maps the highest intensity was such that near-by sidelobes severely distorted the structure surrounding it and such maps have therefore been cleaned (Högbom, 1974; Harten, 1976). The ultimate accuracy to which this cleaning can be pursued is set by the dynamic range in the data (Miley, 1975).

[1] $1\,\mathrm{mJy} = 10^{-3}\,\mathrm{Jy} = 10^{-29}\,\mathrm{W\,Hz^{-1}m^{-2}}$

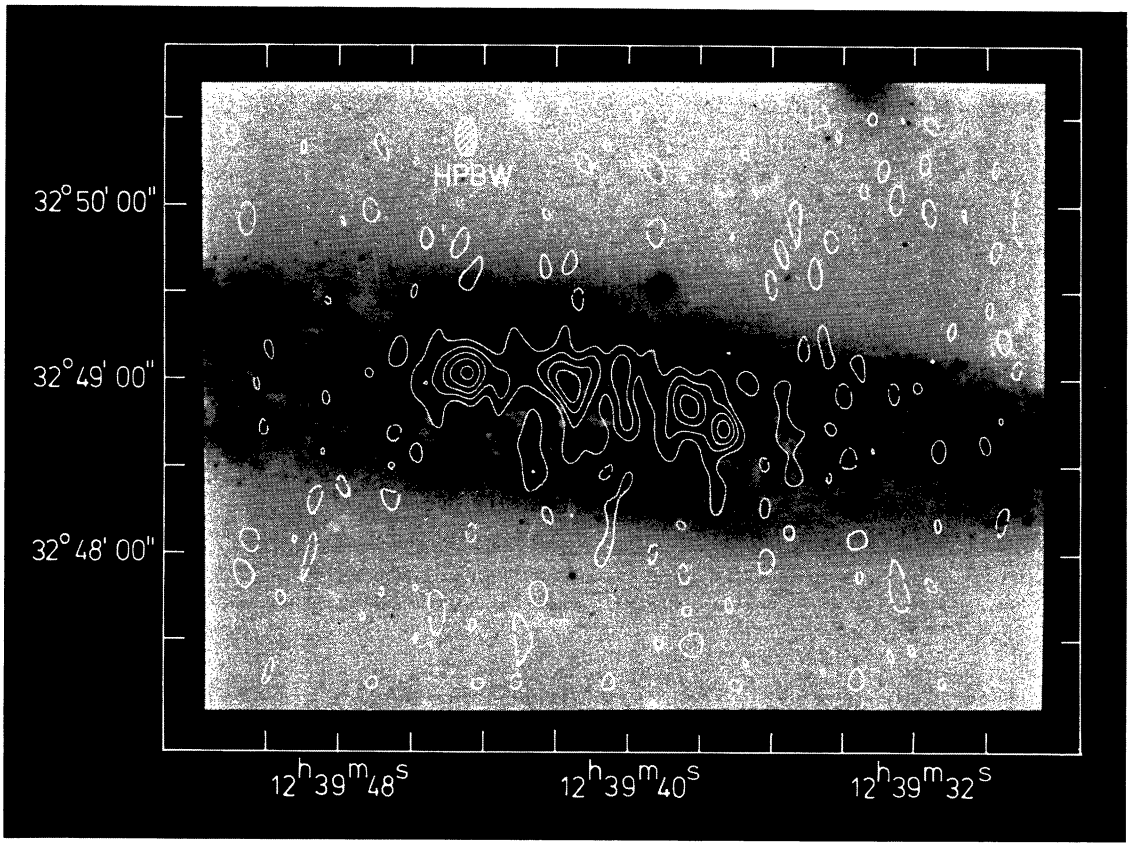

Fig. 1. Full resolution 6 cm map of the central region of NGC 4631 superimposed on an optical photograph (courtesy Hale Observatories). Contours are in units of 1.5 mJy, negative contours are dashed and the zero is omitted. The r.m.s. noise is 0.75 mJy

To determine the spectral properties of extended emission observed at two or more frequencies the data at the higher frequency was convolved to the resolution of the lower frequency data. The successive steps employed in such a spectral comparison have been described by de Bruyn (1977).

All observed brightness distributions are displayed as contour maps, often super-imposed on optical photographs. Accurate positions of reference stars used for such superpositions were measured by Mr. A. Schoenmaker using the Palomar Observatory Sky Survey prints and SAO standards. The final overlays are accurate to $1-2''$. All positions in this paper refer to epoch 1950.0. In the presentation of contour maps, non-linear contour stepping intervals are often used in order to display details in both high and low-brightness features.

3. NGC 4631

NGC 4631 is a late type galaxy seen nearly edge-on. It was classified as Sc by Hubble and as a Magellanic-type (barred) spiral by de Vaucouleurs and de Vaucouleurs (1963). The galaxy appears somewhat distorted which may be due to interaction with NGC 4656/57 which is at an angular separation of 40′. In the following we will adopt a distance of 5.2 Mpc (Sandage and Tammann, 1974) corresponding to a scale of 25 pc/1″.

Previous high-resolution radio continuum observations (Pooley, 1969; van der Kruit, 1973a) indicated the presence of a triple radio structure near the centre of the galaxy on top of a bright disk component. This structure will be further investigated in this paper.

3.1. 6 cm *Observations*

A full resolution 6 cm map of NGC 4631 is shown in Figure 1. Only the central region of the galaxy shown there is bright enough to stand out above the noise, although it should be realized that structure larger than about 5′ in the EW-direction, would not be reproduced in this map (it being larger than the grating ring separation). Such structure is present in the galaxy and, in fact, accounts for the larger part of the flux density of NGC 4631. The triple structure visible at 21 cm now clearly breaks up into at least five components and it is unclear which, if any, is to be identified with the nucleus of the galaxy. The ratio of surface brightness in the complex central structure to that of the large scale disk emission is about twenty. This value is based on a spectral index for the disk component of -0.7 between 6 and 21 cm (this being the value observed between 21 and 49 cm by Ekers

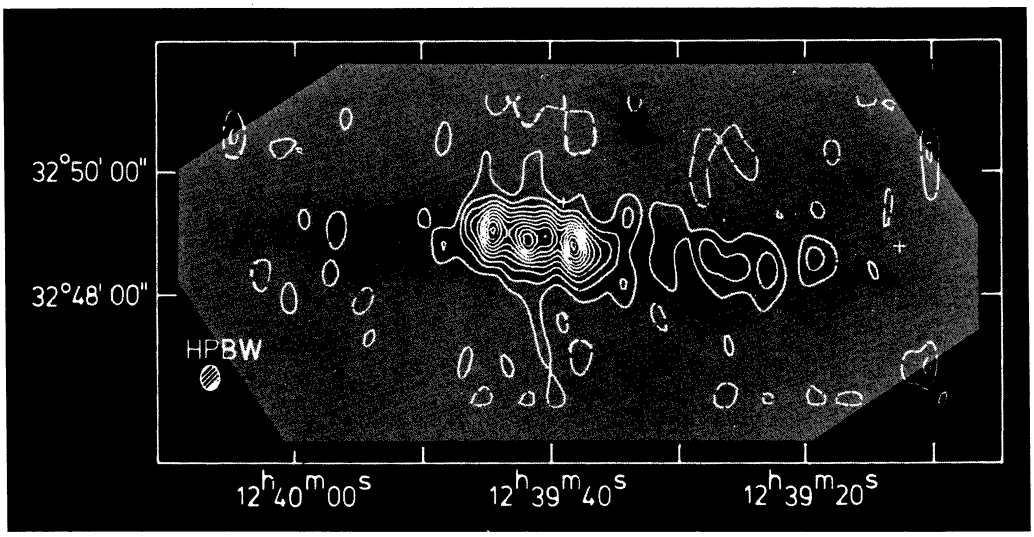

Fig. 2. 6 cm map of NGC 4631 convolved to a resolution of 18″ × 33″ superimposed on a blue optical photograph. Contours are in units of 2.5 mJy, negative contours are dashed and the zero is omitted. The r.m.s. noise is 1.3 mJy. No correction for primary beam attenuation has been applied in the map. The crosses indicate stars used for positioning

and Sancisi (1976); spectral index defined as $S \propto \nu^{\alpha}$). The spectral index of the central complex has been determined by convolving the 6 cm data to the 21 cm resolution and allowing for the different sensitivities to extended structure[2]. In the convolved 6 cm map we can again distinguish three components which have spectral indices of -0.58 ± 0.05, -0.62 ± 0.05 and -0.50 ± 0.05 (from east to west). These are about equal to the value between 21 and 49 cm for the central complex plus disk (Ekers and Sancisi, 1976). Since the spectrum is straight over such a large frequency range most of the emission from the central complex must be nonthermal.

Figure 2 shows a convolved map superimposed on a short exposure blue photograph kindly provided by Dr. G. de Vaucouleurs (see de Vaucouleurs and de Vaucouleurs, 1963). This map shows several regions of weak emission in the western part of the galaxy which were absent on the full resolution map; they must therefore have angular dimensions of 10″ or more. Since they do not show up as clearly on van der Kruit's and Pooley's map they probably have a flatter spectrum than the underlying disk. They coincide approximately with some of the brightest H II regions in NGC 4631 (Crillon and Monnet, 1969) and they are therefore likely to be thermal.

Upper limits of about 15% (3σ) are set to the linear polarization of each of the three components of the central complex after convolving the data to the 21 cm beam.

[2] In van der Kruit's observations, taken at a frequency of 1415 MHz, some contamination is present from neutral hydrogen in the galaxy whose signal falls near the half-power point of the 4 MHz bandpass. This, however, causes no error in the spectral index because the contamination changes only slowly in magnitude under the central complex. This has been checked with the new 1410 MHz observations by Ekers and Sancisi (1976)

3.2. Discussion on the Central Complex

Pooley and van der Kruit both raised the possibility that the central emission complex is due to a pair of inner spiral arms seen tangentally. To test this conjecture, van der Kruit compared the brightness profile of NGC 4631 with that of M 51 if the latter were seen edge-on. A similar comparison between NGC 891, M 31, NGC 4631 and our own galaxy is given in Baldwin and Pooley (1973). Since the differences remain appreciable we will assume that the structure is confined to the central region, has a line-of-sight depth equal to the lateral extension and is due to an additional component of radiation over the base disk. The corollary is that the synchrotron emissivity in the central complex, compared to that in the surrounding disk, must still be an order of magnitude higher than the ratio of surface brightnesses. This enormous increase in volume emissivity implies that the magnetic field energy density and the relativistic electron density must each be more than an order of magnitude higher (their ratio assumed fixed) in the central complex. A possible cause of this increase is discussed further in Section 7.

4. NGC 4258

This galaxy (Type Sb) is the best studied optically of the four (see van der Kruit, 1974 and references therein). In the following we adopt a distance of 6.6 Mpc as determined by Sandage (cf. Burbidge et al., 1963) at which distance 1″ equals 32 pc. NGC 4258 appears to be an isolated system except for a nearby dwarf galaxy NGC 4248.

We have observed NGC 4258 at wavelengths of 6 and 49 cm. Combining these data with the earlier 21 cm

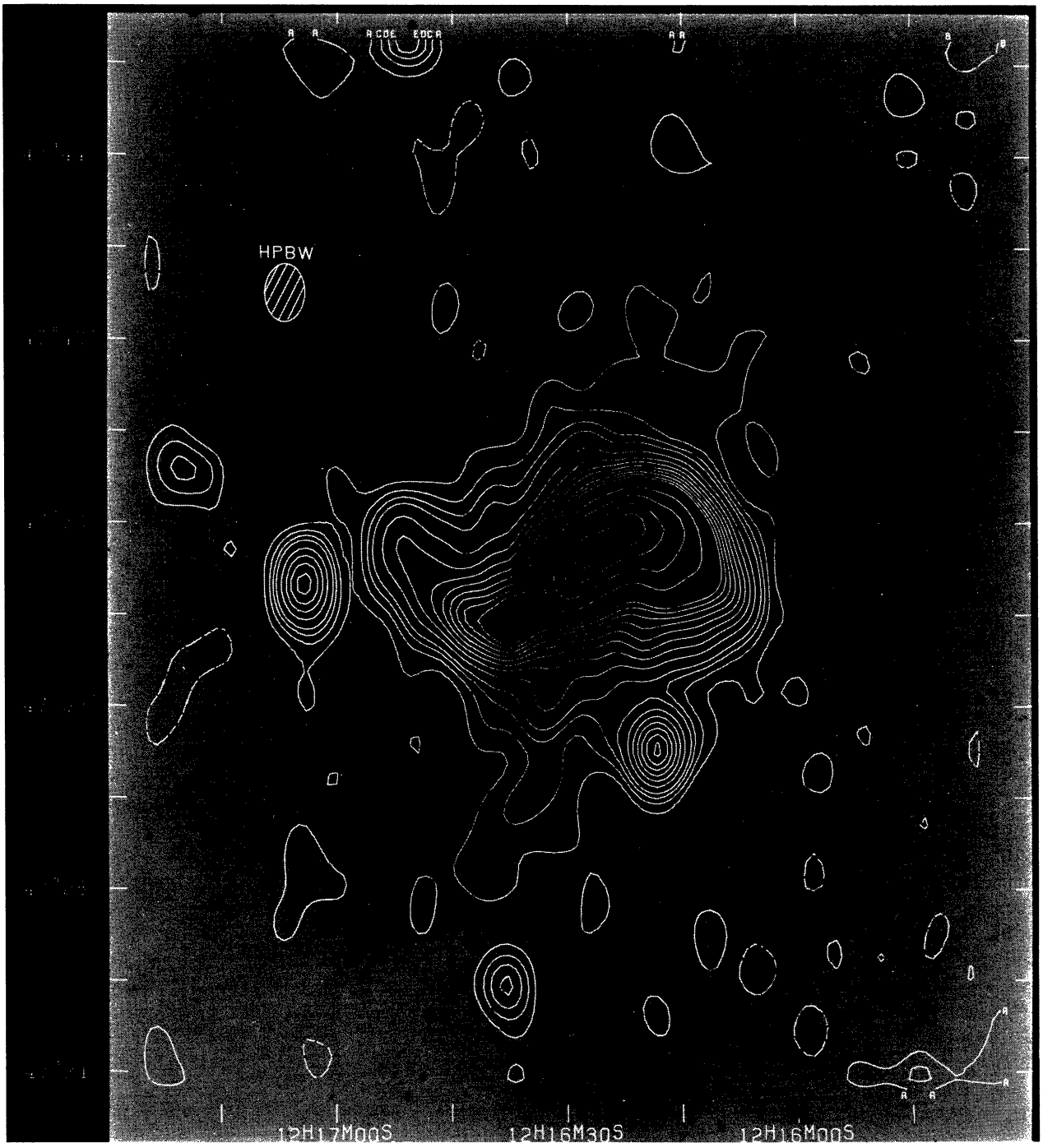

Fig. 3. Contour map of the 49 cm emission of NGC 4258 (cleaned and restored with a Gaussian beam) superimposed on an optical photograph (courtesy Hale Observatories). Contour values are −2.5, 2.5 (2.5) 10 (5) 50 (25) 150 mJy, the negative contour is broken. The r.m.s. noise is 1.3 mJy. Letters at the edges are symbols used in the plotting program for contour identification

measurements (van der Kruit et al., 1972, henceforth KOM) allowed us to study the spectral index distribution.

4.1. 49 cm *Observations*

A contour map of the 49 cm emission is shown in Figure 3 superimposed on an optical photograph. In addition to the emission of NGC 4258 five discrete background sources can be seen. The improved signal-to-noise ratio compared to the 21 cm map leads us to the following comments (we assume that the reader is familiar with KOM).

i) The emission from the so-called anomalous radio spiral arms terminates *abruptly* at about 4′ east and west of the nucleus. Apart from intensity differences the

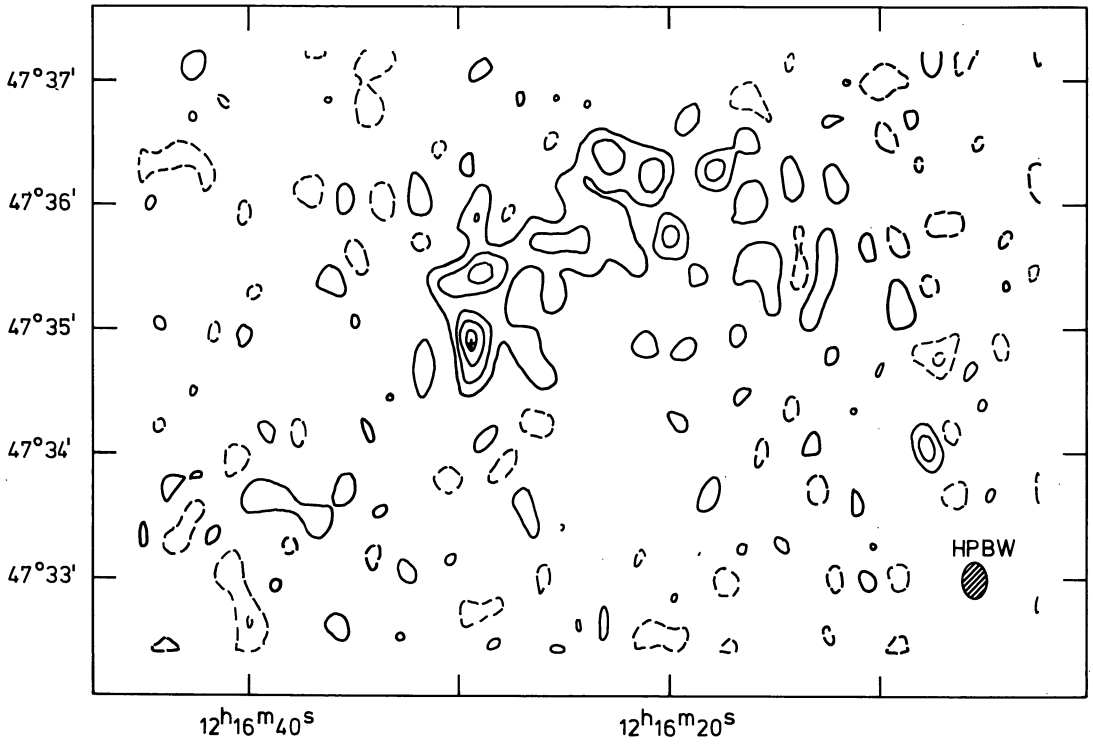

Fig. 4. Contour map of the 6 cm radio emission of NGC 4258 convolved to a resolution of 12″ × 16″. The position of the optical nucleus is indicated by a + sign. Contour values are in units of 1.75 mJy, negative contours are dashed and the zero is omitted. The r.m.s. noise is 1 mJy. No correction for primary beam attenuation has been applied

eastern and western branches are very symmetric. The endpoints of the radio arms mark the edges of the optical emission as determined from a stack of three deep plates taken by Arp with the Kitt Peak 4 m telescope. More interesting perhaps is the fact that the radio arms also mark the edges of the neutral hydrogen distribution (van Albada and Shane, 1975) since the radial decrease of radio continuum brightness is more compatible with the H I surface density profile. This is the strongest evidence for the radio arms being in the plane of the galaxy (for some other arguments see KOM).

ii) Weak emission can now be detected in regions away from the anomalous arms and their associated plateaux. The southern optical arm, for example, shows up clearly although many of the other optical spiral features do not appear above a level of 2 K brightness temperature. The average surface brightness of the anomalous arms at 49 cm is about 100 K, taking into account that they are only marginally resolved, implying that the ratio of surface brightness in the anomalous arms to that in the normal spiral arms is of the order of 100.

iii) There is no apparent connection with any of the background sources only a few of which are seen in Figure 3. Note, however, the weak source at position ($12^h17^m20^s$, +47°37′) which falls on the line connecting the optical nucleus with the tip of the eastern radio arm and is extended in the same direction. No obvious optical counterpart was found. An interesting optical identification was found for the bright extended source near the tip of the eastern arm. De Ruiter et al. (1976) discovered close to the radio centroid an optically variable QSO. No emission stronger than 4 mJy was detected from NGC 4248.

iv) The polarized emission is less than 3 mJy everywhere except at one position ($12^h48^m51^s$, +47°34′50″) near the end of the eastern arm where we measured 4 ± 1 mJy with the electric vector in position angle $85 \pm 15°$. If real, it corresponds to $23 \pm 6\%$ linear polarization[3]. The limit to the percentage polarization at the brightest part of the western arm is 2% (3σ).

4.2. 6 cm *Observations*

On the full resolution 6 cm map the highest peak of 4 mJy was detected at the position of the optical nucleus. This emission is definitely extended and we estimate 3 mJy to be an upper limit to the flux density of a point source in the nucleus. Even in the convolved map shown in Figure 4 the signal-to-noise ratio remains low and the eastern arm still does not show up. The western arm is resolved in the backwards direction (the rotation being anti-clockwise) as was already apparent from the 21 cm data. The S/N ratio is insufficient to make any statements on the steepness of the leading edge. On a map convolved to

[3] New more sensitive observations at 21 cm confirm the reality of the linear polarization at that position (van Albada, private communication)

a resolution of $45'' \times 61''$ no linear polarization was detected above a level of 6 mJy per beam area (3σ) which implies a linear polarization less than 20% at the brightest part of the western arm.

4.3. Radio Spectral Index Distribution

We have determined the spectral index distribution between 21 and 49 cm and between 6 and 21 cm, both with a resolution of 56". The results for the 21/49 cm comparison are shown in Figure 5. The values are sampled at intervals about one beamwidth apart. The large errors on the eastern side are due partly to some weak instrumental effects around the field centre in the convolved 21 cm data. No significant changes from a value of about -0.60 are observed along the ridges of the anomalous radio arms but the plateau to the south of the western arm has a steeper spectral index. An even steeper spectral index ($\alpha < -1.25$) is derived for the emission from the outermost south western spiral arm. On the other hand, the relatively bright optical arm south of the nucleus containing the string of HII regions (cf. Fig. 2 in KOM) has a much flatter spectrum. This apparently contradicted the fact, noted by KOM, that the radio emission from this arm coincides with the dust rather than the string of HII regions. After analyzing the accuracy of the superposition it appears that their radio map must be shifted slightly westwards with respect to the optical photograph. The radio emission then coincides with the HII region string and is therefore likely to be thermal. In the 6/21 cm comparison there are only a few beam areas where a reliable value for the spectral index can be determined. In the region from the nucleus up to about 3′ along the western arm we find $\alpha = -0.8 \pm 0.1$ with a somewhat flatter value of -0.6 slightly north-east of the nucleus. The contamination by thermal radio emission in this area is probably not insignificant and the nonthermal component may therefore have a steeper spectral index than these values indicate.

The integrated radio spectrum of NGC 4258 is poorly determined. Assuming that there is no structure larger than 15′ we derive flux densities of 0.82 ± 0.05 Jy at 21 cm and 1.39 ± 0.10 Jy at 49 cm from summation of the components found in the clean routine. The 21 cm value agrees well with those reported by KOM (determined from contour planimetry), Lequeux (1971) and Maslowski (1972). Flux density determinations at other wavelengths are uncertain; the values given by de Jong (1967) and Kazès et al. (1970) at 11 cm differ considerably which may be due to resolution effects. Similarly the 6 cm flux density determined by Sramek (1975) is probably too low because he observed with a 5′ beam but detected no beam broadening.

4.4. Magnetic Field and Total Energy Calculations

The polarization data has yielded little or no information on the magnetic field structure in the anomalous radio arms. The absence of linear polarization can, however, be ascribed to Faraday depolarization along the line-of-sight if one assumes a magnetic field strength of 10^{-5} G (see below), a thermal electron density of 1 cm^{-3} and an inclination corrected depth of 600 pc. For this plausible set of parameters even a completely uniform magnetic field would yield a degree of polarization less than the observed limits (e.g. Burn, 1966).

The magnetic field strength of 10^{-5} G used above has been computed on the assumption of energy equipartition between magnetic field and relativistic particles (equal energy in protons and electrons) and a z-thickness of the radio arms of 200 pc. Subject to these assumptions, the total energy in the radio arms is a few times 10^{54} erg.

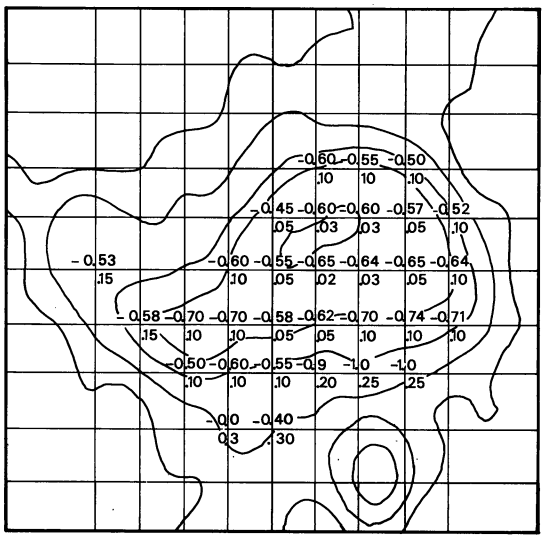

Fig. 5. Spectral index distribution between 21 and 49 cm for NGC 4258. The spectral indices and their $\pm 1\sigma$ errors are given at intervals of 5^s in right ascension and 1′ in declination and are superimposed on some of the contours of Figure 3

5. NGC 2146

NGC 2146 is a peculiar spiral galaxy of type Sap first studied by Pease (1920). De Vaucouleurs (1950) has drawn attention to a peculiar dust structure crossing the central region of the galaxy just west of the nucleus and to which he refers as "the third arm". Spectroscopic and photometric observations have been made by Burbidge et al. (1959), Benvenuti et al. (1975) and Cheriguène (1975). The galactocentric velocity of the galaxy is about 1050 km s^{-1} from which we derive a distance of 21 Mpc corresponding to a scale of 102 pc/1".

5.1. 21 cm *Observations*

A contour map of the 21 cm emission is shown in Figure 6 superimposed on an optical photograph taken with the Mount Ekar 182 cm reflector (courtesy Dr. S. D'Odorico). The noise level in the map is set by the dynamic range in the data, which is determined by

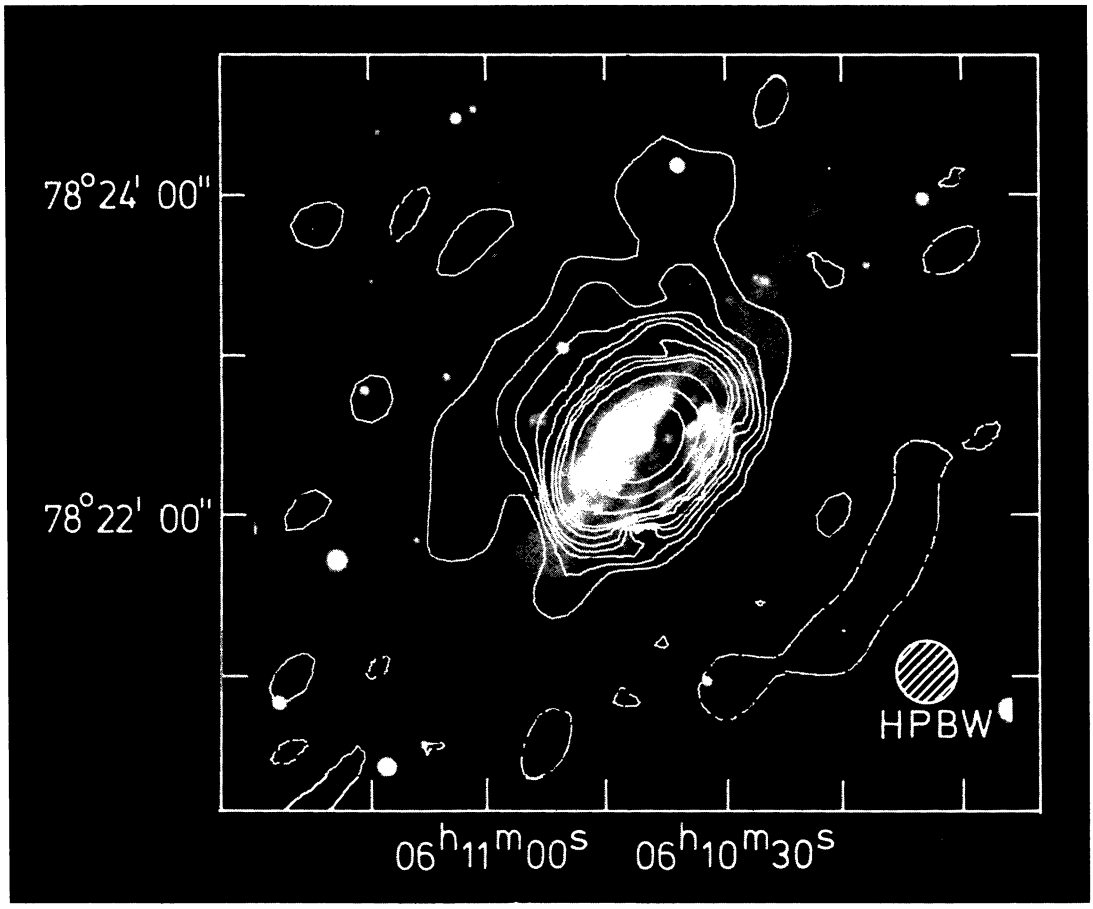

Fig. 6. Map of the 21 cm emission of NGC 2146 (cleaned of the effects of near-in sidelobes) superimposed on a blue photograph. Contour values are −4, −2, 2(2)10(5)25, 50, 125, 250, 500 mJy, the negative contours are dashed. The noise level is about 1–2 mJy (see text)

atmospheric gain and phase fluctuations, rather than the thermal noise which is 0.4 mJy. The dominant structure is an unresolved ridge of emission in position angle 126° responsible for 80—85% of the total flux density. Surrounding this ridge is a region of about 1.5′ diameter with a surface brightness of 10—20 K and some faint spurs to the east and north, together containing some 15—20% of the galaxy's flux density. No emission stronger than 2 mJy per beam area (2.4 K) has been detected from the outer spiral arms. No linear polarization in excess of 2 mJy has been detected corresponding to less than 0.5% at peak brightness.

5.2. 6 cm *Observations*

A contour map of the 6 cm emission is shown in Figure 7. Due to instrumental failure we had to delete the two shortest baselines in the Fourier inversion of the data. Because of these missing short spacings the 1.5′ structure seen at 21 cm is not represented in this map (anyway, its surface brightness is too low to record it even if we did have the short baseline information). The ridge described in the 21 cm analysis is found to be still unresolved although some faint emission is detected on either side of it. The emission seen in the 6 cm map accounts for 80% of the total flux density. From the very smooth and symmetric brightness profile in position angle 126° we derive an upper limit of 15 mJy to the flux density of a compact nuclear source. The width of the narrow ridge dominating Figure 7 has been estimated from the normalized fringe visibility curve in position angle 36° (fringes parallel to the ridge) which is shown in Figure 8. From this curve we find that at the longer baselines the emission is due to a source with a half width of 2″ or less still containing 30% of the total flux density of the galaxy. Because the narrow part of this ridge extends to about 15″ on either side of the nucleus, the ridge can not be explained as a circularly symmetric disk in the equatorial plane for which we adopt an inclination angle of 55° (Danver, 1942). On the other hand, the faint emission on either side of the ridge and the 1.5′ structure visible at 21 cm will appear approximately circular when the galaxy is viewed face-on. If the radio ridge is in the plane of the galaxy it must therefore be highly elongated. No linear polarization has been detected at 6 cm above a level of 3 mJy (3σ) which equals 4% at peak brightness.

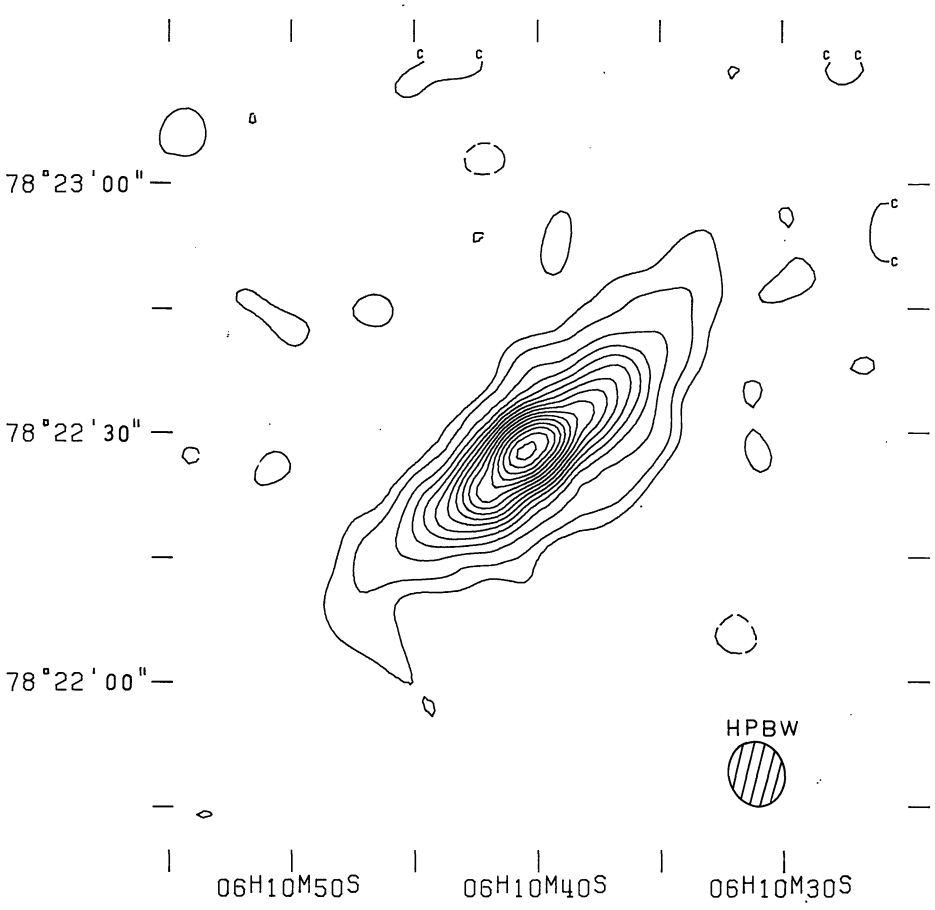

Fig. 7. Map of the 6 cm emission of NGC 2146 (cleaned of the effects of near-in sidelobes). Contour values are −2.5, 2.5, 5 (5) 75 mJy, the negative contour is dashed. The r.m.s. noise is 1.2 mJy. Letters at the edges are used by the plotting program for contour identification

5.3. Radio Spectrum and Miscellaneous Points

Due to the missing large scale structure in the 6 cm map we have not attempted to determine the spectral index distribution between 6 and 21 cm. The integrated flux density is 0.475 ± 0.025 Jy at 6 cm, and 1.08 ± 0.03 Jy at 21 cm. For a spiral galaxy the unusual intensity and compactness allowed a good integrated spectrum to be determined. This is shown in Figure 9 where a single power-law with $\alpha = -0.62$ is seen to fit the data extremely well. We note here that, even at the highest frequencies, the radio emission is likely to be predominantly non-thermal. The giant spiral galaxy M 101, for example, which is very rich in HII regions, would only have a thermal flux density of 10 mJy at the distance of NGC 2146 (Israel et al., 1975).

At position ($06^h10^m02^s.0, +78°17'09''.4$) we detected a bright unresolved ($<3''$) radio source with flux densities of 160 ± 25 mJy at 6 cm, and 142 ± 3 mJy at 21 cm. The source is linearly polarized by $3.5 \pm 0.4\%$ at 21 cm with the electric vector in position angle 51°. From the continuum channels of unpublished 21 cm line observations of NGC 2146 there are indications that the source is variable. We have tentatively identified it with a faint ($m_B \sim 20$) stellar object on the photograph provided by Dr. D'Odorico. We mention it here because of its interesting properties and the fact that it confuses pencil beam observations of the galaxy. No emission stronger than 4 mJy was detected from NGC 2146A, which is situated 20′ north-east of NGC 2146.

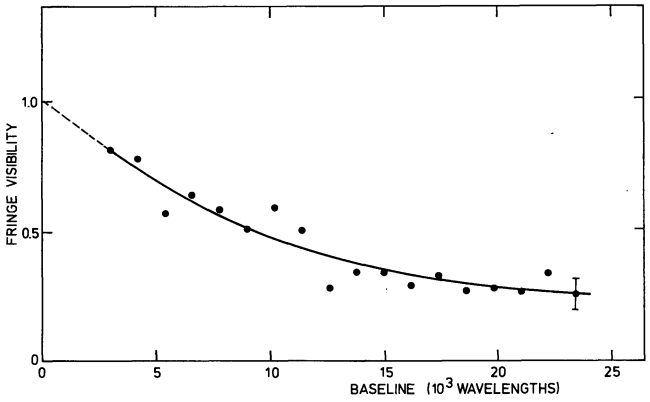

Fig. 8. Fringe visibility curve of NGC 2146 in position angle 36° (averaged over 5° in position angle). The $\pm 1\sigma$ error bars are shown on the longest baseline data point. The extrapolation to zero spacing is based on short baseline data in that part of the U–V plane where instrumental effects are unimportant

A typical brightness temperature at 6 cm in the radio ridge is 50 K which converted to 21 cm corresponds to 1400 K. The brightness contrast between the ridge and the base disk is therefore a thousand or more. If we make

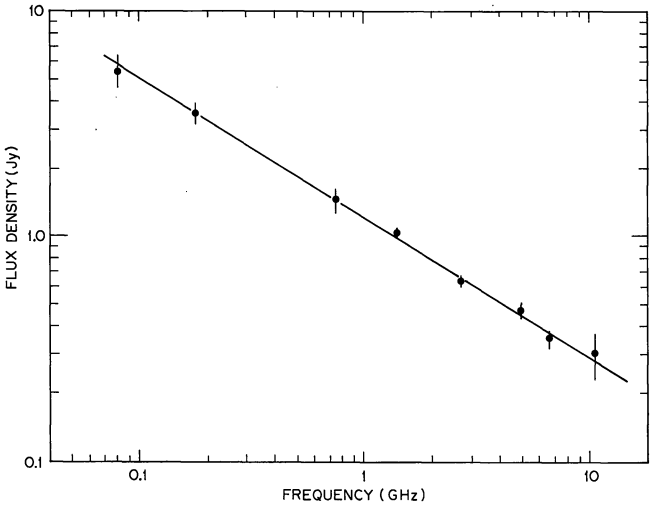

Fig. 9. Spectrum of the integrated radio emission of NGC 2146. At each frequency only the weighted mean flux density is plotted. Flux densities have been taken from this paper, Branson (1967), Gower et al. (1967), Heeschen and Wade (1964), Lequeux (1971), de Jong (1967), Wardle and Sramek (1974), Kaźès et al. (1970), Le Squéren and Crovisier (1974) and McCutcheon (1973). The value at 750 MHz by Heeschen and Wade (1964) has been corrected by 0.2 Jy for the nearby confusing source. The flux densities at 81.5 and 178 MHz have been revised upwards by 15% and 10% respectively, to bring them in agreement with the KPW scale (Véron et al., 1974; Scott and Shakeshaft, 1971)

the simplifying assumption that the ridge has a length of 40″ (4 kpc) and a diameter of 5″ (500 pc) we derive an equipartition magnetic field strength of $5\,10^{-5}$ Gauss (equal energy in protons and electrons) and a total nonthermal energy of about $2\,10^{54}$ erg; a similar value is found for the surrounding 1.5′ (9 kpc) structure.

6. NGC 3079

The almost edge-on galaxy NGC 3079 is the least studied of the four galaxies described in this paper. The classification as a late type spiral (Sc) by Hubble is confirmed by the large neutral hydrogen content and the optical and radio kinematic properties (Gouguenheim, 1969; Roberts, 1968; Baranne et al., 1974). The inclination as measured by Danver (1942) is 83° but this value must be regarded as uncertain because of the irregularity of the outer optical isophotes. It appears that the galaxy is severely distorted if we compare its images on the Palomar Observatory Sky Survey prints and Figure 10 with photographic images of other edge-on galaxies (e.g. Sandage, 1961). In this respect it is interesting to note that NGC 3079 is an isolated system except for two nearby dwarf galaxies. One of these is NGC 3073 (alias Markarian 131), which has the same redshift as NGC 3079 (Huchra, 1976). The galactocentric systemic velocity of NGC 3079 is $+1250$ km s^{-1} and we will adopt a distance of 25 Mpc which yields a scale of 120 pc/1″.

6.1. 21 cm *Observations*

Figure 11 shows the 21 cm map superimposed on the long exposure photograph shown in Figure 10. As in the case of NGC 2146, the noise level close to the central peak is set by the dynamic range in the data and decreases at larger distances. The central peak is for a large part due to a central source (see the 6 cm data below). From an analysis of the fringe visibility curves in several position angles, and comparison with similar curves at 6 cm, we deduce a flux density of the core source of 160 ± 15 mJy. Besides this bright central source there are several interesting features in this map. First, there are extensions from the central source to the east and west which, when deconvolved for the beam size, do not reach further than the edges of the optical disk. Second, there are intense symmetric unresolved ridges along the major axis that reach to about 1′ from the nucleus (1/3 of the semi-major axis). The brightness temperature of these ridges is at least 50 K which is much higher than the underlying disk component which has a width comparable to the galaxy's minor axis. Third, there is a spur of emission to the north that lies on the west side of the galaxy where the optical emission is also brightest. There is no indication of any significant radio continuum halo although there are two faint protrusions from the plane which reach to projected heights of about 5 kpc from the plane. No emission stronger than 2 mJy was detected from NGC 3073 or the anonymus galaxy located to the north-west of NGC 3079.

6.2. 6 cm *Observations*

A map of the 6 cm emission is shown in Figure 12. From an analysis of the fringe visibility curves in several position angles we conclude that there is an unresolved source ($<2''$) at position ($09^h58^m35^s.04 \pm 0^s.06$, $+55°55'15''.7 \pm 0''.5$) with a flux density of 102 ± 5 mJy which lies near the optical centroid of the galaxy. An optical nucleus itself is invisible, even on the short exposure photograph. Although the core source was subtracted from the map, there remained a large amount of slightly resolved emission near its position, the structure of which will undoubtedly change if the derived core position is in error by only a fraction of the beam diameter.

One of the most striking features of the 6 cm map is the cross structure already hinted at in the 21 cm data. The eastern extension of this cross reaches to the edge of the optical disk while the western extension reaches to only about 2/3 of the semi-minor axis, although this may be an artifact of the lower S/N ratio in the western extension. Whatever their origin, it seems reasonable to assume, in view of their symmetrical location, that they have a common origin. Since the E-extension at least covers several beam areas both extensions should prob-

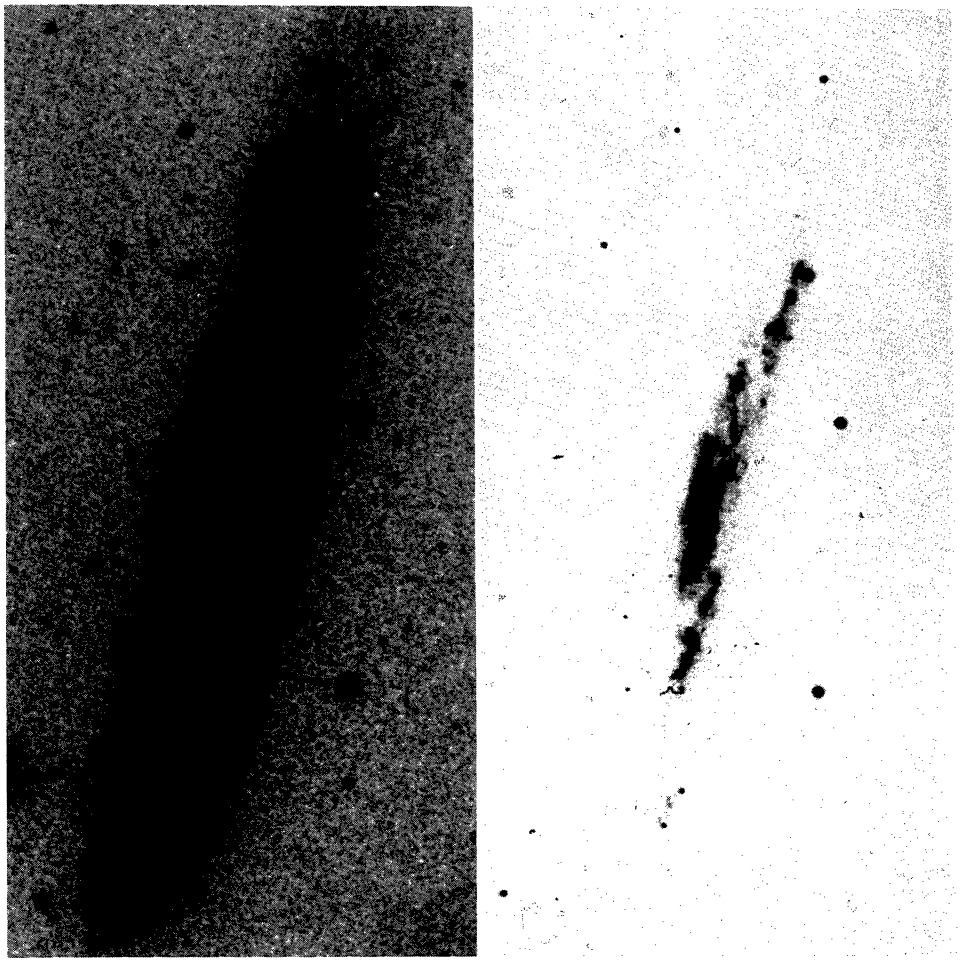

Fig. 10. Left: 1-h exposure of NGC 3079 on IIIa-J emulsion with the 48″ Schmidt at Palomar Observatory (courtesy Dr. H. C. Arp). Right: 15-min exposure on 103a–O emulsion with the Mount Ekar 182 cm reflector (courtesy Dr. S. D'Odorico). The scale on both prints is 4.03″/mm. North is up, east to the left

ably be regarded as a continuous structure and not as a series of discrete sources lined up in a highly inclined disk. If the EW-extensions are perpendicular to the disk they must reach heights of several kpc above the plane and would represent the first case of a spiral galaxy with a double radio source outside its optical boundaries. However, there are several reasons why we think that they are confined to the plane: 1) The extensions do not appear to go further than the projected optical boundaries. Unless this is purely a coincidence the same argument as used for NGC 4258 [Section 4.2i] applies. 2) The ridge of the E-extension curves in the same sense as the (unseen) spiral arms; note that the west side of the galaxy is nearest to us and the north side of the galaxy is approaching (private communication with Dr. D'Odorico). 3) Intense radio ridges also appear in the north-south direction and there is no doubt that they are confined to the plane. If the EW-extensions are indeed confined to the plane they must be emerging almost radially from the nucleus and have a width of 1—2 kpc and a length of 10—20 kpc.

Regarding the NS-extensions we note furthermore that they are much narrower than the minor axis ($<10''$ versus $60''$) which suggests, although not as convincingly as in the case of NGC 2146, that they too are more readily explained as elongated structures emanating from the nucleus than as a highly inclined axially symmetric disk in the inner part of the galaxy. They extend to 6 kpc from the nucleus.

6.3. Radio Spectrum

In most position angles the core source is the only component left at baselines longer than 8000 wavelengths (our longest baseline measures 24000 wavelengths). This core source appears to be still unresolved at baselines of about 50000 wavelengths (Haynes and Sramek, 1975) implying a size less than 1.5″ (180 pc). All published data pertaining to this core source are collected in Table 2. These data yield a spectral index of -0.4 ± 0.1 assuming no variations have occurred.

The small number of beam areas covered by the source at 6 cm, after convolution to the 21 cm beam, and the bright central source render it difficult to determine a reliable spectral index distribution for the NS and EW structures. Their spectral properties were therefore de-

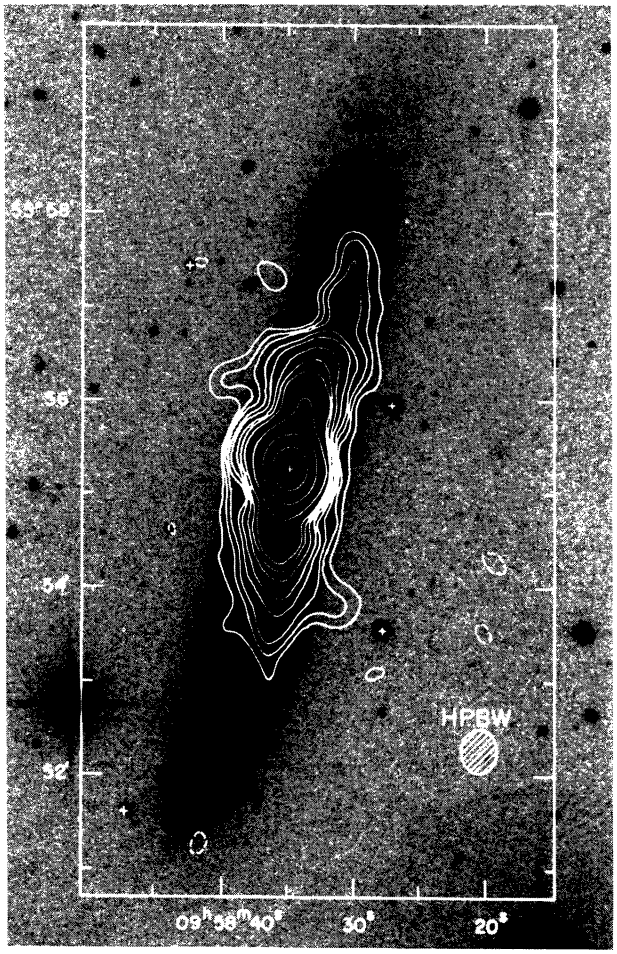

Fig. 11. Map of the 21 cm emission of NGC 3079 (cleaned of the effects of near-in sidelobes) superimposed on the long exposure photograph shown in Figure 10. Contour values are −2.5, 2.5, 3.75, 5 (2.5) 10 (5) 25, 50, 125, 250 mJy, the negative contour is dashed. The peak flux density is 350 mJy. The noise level varies from about 2 mJy close to the central peak to less than 1 mJy elsewhere (see text). The cross in the center indicates the position of the 6 cm radio core, the other crosses indicate stars used for positioning

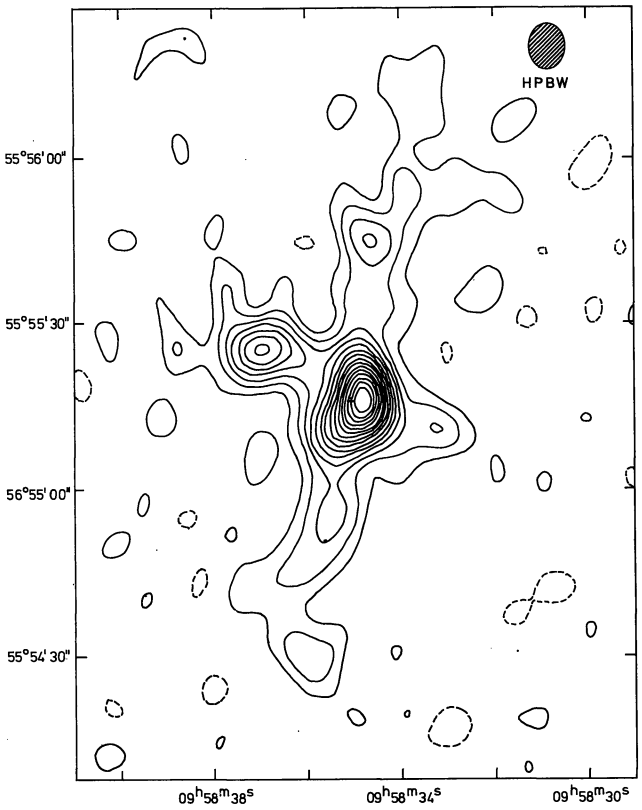

Fig. 12. Contour map of the 6 cm emission of NGC 3079 in the inner part of the galaxy. The cross marks the position of the core which was subtracted from the map. Contour values are in units of 1.5 mJy, negative contours are dashed and the zero is omitted. The noise level is about 0.8 mJy

Table 2. Flux density data for the core of NGC 3079

Frequency (MHz)	Flux density (mJy)	Epoch	Ref.
1410	160±15	1975.5	This paper
2695	105±20	1971–1972	Haynes and Sramek (1975)
2695	~ 70	~1973	Wardle and Sramek (1974)
4995	102±5	1974.3	Unpublished WSRT data
4995	102±5	1975.0	This paper
8085	60±12	1971–1972	Haynes and Sramek (1975)

rived using a different approach which is based on the fact that the source structure is fairly simple in terms of its response in the Fourier transform plane. In position angles 80° and 150°, for example, the contributions from the NS and EW structures in the fringe amplitude curves can be clearly separated (the response of the central source being known already). This somewhat crude analysis indicates that the emission distributed mainly in the EW-direction has a flatter spectrum, $\alpha = -0.6 \pm 0.15$, than the NS oriented component which has $\alpha = -0.95 \pm 0.2$. The total flux density of the galaxy is 0.85 ± 0.03 Jy at 21 cm, of which about half is contained in the NS-extensions and base disk, and 0.350 ± 0.025 Jy at 6 cm. The integrated spectrum is shown in Figure 13. The data seem well fitted by a single power-law with $\alpha = -0.73$, however the two component models suggested above could give an equally good fit to the points. As in the case of NGC 2146 it seems unlikely that thermal radio emission is of any importance in the considered frequency range.

6.4. Linear Polarization, Comparison with Other Spirals and Total Energy Content

At 6 cm, weak linear polarization (at the 4σ level) was detected close to the central peak and on the eastern extension. At 21 cm the central peak is polarized by 0.5% but this is close to the instrumental polarization. Weak (4σ) polarization at 21 cm was also detected about 1′

north of the nucleus. All these polarization results must be considered marginal but we note that Wardle and Sramek (1974) also detected weak linear polarization. The anomalous character of the radio emission in NGC 3079 becomes apparent when we compare its stepwise decrease in intensity with the smooth brightness profiles found for NGC 891, M 31 or our own galaxy (Baldwin and Pooley, 1973). This is obviously due to the fact that we are not seeing the base disk component in NGC 3079. This base disk is estimated to have at most about 1% of the brightness of the EW and NS-extensions.

The volume of the radio emitting structures is difficult to estimate because of the large inclination of the galaxy. Assuming the orientation suggested in Sections 6.1 and 6.2 and assuming that z-extensions are no larger than a few hundred pc we deduce an equipartition magnetic field strength of several times 10^{-5} Gauss and a total energy of about 10^{55} erg, quite similar to the values deduced for NGC 4258 and NGC 2146.

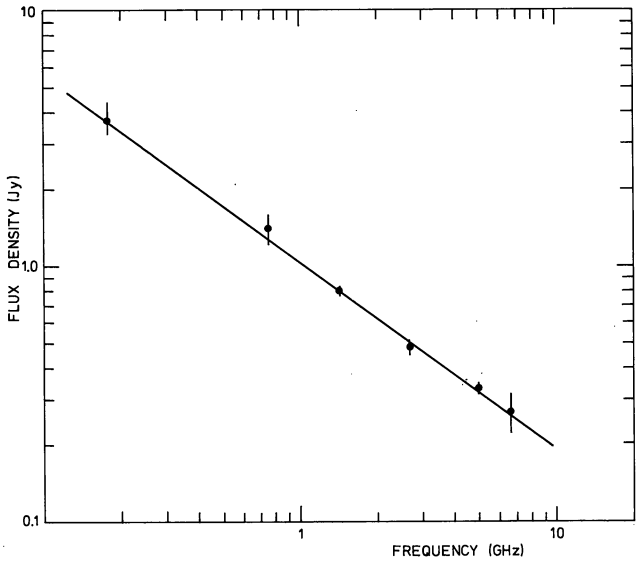

Fig. 13. Spectrum of the integrated radio emission of NGC 3079. At each frequency only the weighted mean flux density is plotted. Flux densities were taken from this paper, Gower et al. (1967), Heeschen and Wade (1964), de Jong (1966), Lequeux (1971), Kazès et al. (1970), de Jong (1967), Le Squéren and Crovisier (1974), Sramek (1975) and McCutcheon (1973). The 178 MHz value has been revised upwards by 10% to bring it in agreement with the KPW-scale (cf. Véron et al., 1974; Scott and Shakeshaft, 1971)

7. Origin of the Radio Structures

In this discussion we will attempt to explain the following three properties that the anomalous radio structures of these four galaxies have in common:

1) The radio structures have no obvious relation to normal optical structures (neglecting such special features as the H_α-arms in NGC 4258).

2) They combine a high degree of symmetry with respect to the nucleus with a fair degree of collimation in the azimuthal direction (for at least three of them).

3) Their surface brightness is extremely high, both compared to their own disk and spiral arm emission as well as to the disks of other spiral galaxies (van der Kruit, 1973c).

In an attempt to learn more about their origin we first ask ourselves whether these structures are permanent features of these galaxies or whether they are young and evolving. The enormous intensity contrast between the various parts of each galaxy suggests that they are not stationary features. One might expect, for example, that differential rotation would smear these large-pitch-angle structures in less than a few times 10^8 years unless they are the "radio equivalent" of the optical bars in barred spiral galaxies. In the latter case they must be quite different phenomena because barred spirals show no exceptional radio emission from their bars (van der Kruit, 1973b). The radio spectral properties of the four spiral galaxies give us a handle on this problem. All four galaxies have, over the available frequency range, a radio spectrum with $\alpha \approx -0.6$ to -0.7. Below we will use the structure and spectrum of the source in NGC 2146 as our quantitative guide and comment further on how much of the reasoning applies to the other three galaxies.

As shown in Figure 9 the radio spectrum of NGC 2146 can be described by a single power-law with an index -0.62 over more than two decades in frequency. It seems reasonable to assume that this spectral index represents the energy spectrum of the relativistic electrons at their place of origin and that energy loss processes have not effected this spectrum. Otherwise, the electrons must have an exceptionally flat ($\gamma \sim 1.2$, $\alpha \sim -0.1$) or steep ($\gamma \sim 3.2$, $\alpha \sim -1.1$) injection spectrum (e.g. de Bruyn, 1976). According to a well-known argument (e.g. van der Laan and Perola, 1969) the lifetime of the electrons in the source must then be less than a certain value to avoid the appearance of a high-frequency break in the radio spectrum. A similar argument applies to the absence of a low-frequency break (de Bruyn, 1976), but we will not consider it here because it is less restrictive. If we denote by H_r the "equivalent magnetic field strength" to which the radiation losses due to inverse Compton processes on the 2.7 K universal photons and the stellar photons in the galaxy are attributed, and H is the magnetic field in the galaxy (both in Gauss), we find

$$T \lesssim 0.25 H^{1/2}(H^2 + H_r^2)^{-1} \quad \text{years}.$$

The maximum possible value for the age T is obtained for $H = H_r/\sqrt{3}$

$$T_{\max} \approx 0.14 H_r^{-3/2} \quad \text{years}.$$

Any other value of H, lower or higher, will lead to a still smaller age limit according to

$$T \approx 1.8 (H/H_r)^{1/2}\{1 + (H/H_r)^2\}^{-1} T_{\max}.$$

The value of H_r is at least $4\,10^{-6}$G (due to 2.7 K photons only), but since the radio source lies in the very bright

central region of the galaxy in which most of the stellar luminosity is generated (Burbidge et al., 1959) the radiation density of stellar photons will be much larger. We estimate that H_r is at least 10^{-5} G, which yields $T_{max}=4.4\,10^6$ years. If we assume that H equals the equipartition value, T will be only $4\,10^5$ years. In the following we will adopt a maximum age of 10^6 years as a compromise.

If we substitute appropriate values of H_r and H_{eq} for the other galaxies we derive, from the absence of spectral steepening below frequencies of 5 GHz, 1.4 GHz and 6 GHz (for NGC 4631, NGC 4258 and NGC 3079), age limits of a few times 10^6 years, 10^7 years and $5\,10^6$ years, respectively.

How can we reconcile the very small age of the relativistic electrons in NGC 2146 with the observed linear extent? The following two schemes, based on an equilibrium situation and an evolving source model, seem to be the only possible explanations. 1) The particles leak out of the source on a timescale less than 10^6 years. This implies diffusion speeds (sideways or in the z-direction) greater than several hundred km s^{-1}. If the faint emission around the ridge is to be identified with the leakage reservoir, one expects its radio spectrum to be steeper than $\alpha=-0.62$. Unfortunately, our data do not permit a check of this hypothesis. An important consequence of rapid leakage is that to maintain the particle energy density, an electron injection rate of $10^{40}-10^{41}$ erg/s is required. So much energy cannot be provided by supernovae or any other discrete source population in such a small volume of space [the estimated electron energy input from supernovae in our galaxy *as a whole* is about 10^{39} erg/s (Ginzburg, 1974)]. The only plausible sources left are the nucleus of the galaxy or *in-situ* acceleration. If the particles originate in the nucleus they must propagate at bulk speeds greater than 1000 km s^{-1} because the extent of the radio ridge to either side of the nucleus is at least 1 kpc. On theoretical grounds (Wentzel, 1969; Kulsrud and Pearce, 1969; Skilling, 1970) this seems to be excluded unless another constituent is ejected along with the relativistic particles that carries both enough momentum to sweep up or push aside the interstellar gas and inertia to confine the relativistic particles. This can only be provided by large amounts of gas which thus must also move at velocities greater than 1000 km s^{-1}. If particle production occurs in situ, some event must have occurred that has disturbed the interstellar medium simultaneously out to distances of several kpc from the nucleus in opposite directions. Only large amounts of gas seem capable of doing this, which brings us back to the nuclear ejection scheme. However, since in the in-situ acceleration scheme the relativistic electrons themselves are not coming from the nucleus but only their "cause", we can now not put any limits on the velocity with which this "cause" propagates. What could be the physical mechanism that leads to in-situ acceleration? We may have to reconsider the classic Fermi-mechanism operating on the background cosmic rays in the disk. However, it has to be very efficient and very fast because the brightness enhancement over the base disk is a thousand or more and the time scale cannot be longer than 10^6 years. 2) One can avoid the rapid leakage argument and some of its consequences by supposing that the whole phenomenon is younger than 10^6 years. Basically this leads to the same conclusions as in the previous model except that one *has* to assume that the velocity of the gas expelled from the nucleus was larger than 1000 km s^{-1}.

Concluding we can say that in both schemes we are led to the corollary, *on the basis of radio data only*, that there must have been (and may still be) large quantities of gas ejected from the nucleus at speeds possibly as high as 1000 km s^{-1} or more. The radio ridge suggests that this was to a large extent a directed expulsion. The optical structure of the galaxy provides some corroborating evidence for gas expulsion. For example, the peculiar dust structure crossing the central region indicates that a lot of dust, and presumably gas as well, must have been transported to a considerable distance above the plane. It is conceivable that the very large relativistic particle pressure in the central radio source has also played a rôle in lifting gas to large distances above the plane through the Parker instability. Furthermore, there are large amounts of ionized gas in the central region with a rather high velocity dispersion (Burbidge et al., 1959). The "ultimate proof" of gas ejection from the nucleus, the observation of this gas itself, may be difficult to obtain because as soon as the ejected gas hits the interstellar gas it will be shock-heated to X-ray temperatures, become very diluted and virtually unobservable. If the ejected or swept-up gas slows down to velocities of $\lesssim 100$ km s^{-1} it might become detectable but we would not deduce that the velocities are very abnormal. If one assumes a conversion efficiency of kinetic energy into turbulent energy of 1 % (cf. Gull, 1973), the kinetic energy in the in-situ model must have been of the order of $10^{56}-10^{57}$ erg. A similar value is found when one assumes that a considerable fraction of all the gas originally present in the radio ridge must have been accelerated to velocities of about 1000 km s^{-1}.

The model for NGC 2146 presented here bears many similarities to that of KOM for NGC 4258. It is therefore intriguing to learn that NGC 2146 also has a bright H_α-arm emerging from the nucleus (Alloin et al., 1975). This arm underlies the south-eastern half of the radio ridge. A counterpart to the north-west would remain obscured by the dust arm. Regarding NGC 4258 itself, the radio spectral data do not add much support to the KOM model, nor do they contradict it. The age limit of 10^7 years deduced above for the electrons in the radio arms applies to all parts of these arms which extend to some 15 kpc from the nucleus. The "equivalent velocity" that we calculate from these numbers is 1500 km s^{-1}. This is just about equal to the gas ejection velocity in the model of KOM, which is mainly fixed by the geometry of the source. It is therefore not possible to choose between an in-situ acceleration model or a nuclear model for the relativistic electrons. However, since the brightness en-

hancement in the anomalous radio arms in NGC 4258, with respect to that of the base disk, is at most about 100, it is possible that the *present emission* from the radio arms is largely due to to background cosmic ray electrons whose emission is enhanced by nonlinear effects (Cowsik and Mitteldorf, 1974) in a turbulent medium. The apparent steepening of the spectrum on the western plateau when one comes further from the leading edge may indicate that there the turbulence is less strong, leading to weaker emission and radiation-loss effects in the spectrum, or that the plateau is older (as suggested by KOM).

The structure of NGC 3079 is not easily incorporated in the directed explosion models proposed for NGC 4258 and NGC 2146, unless two explosions in orthogonal directions took place. In a way, NGC 3079 combines the structures of the other two galaxies: one fairly compact structure in the inner part of the galaxy and one probably reaching to the edge of the galaxy. The age limit deduced for the relativistic electrons in the anomalous structures in NGC 3079 is a factor of five larger than the corresponding limit for NGC 2146 but since the linear extent of the radio extensions is larger by a similar factor the equivalent velocities are the same. Evidence for nuclear activity in NGC 3079 comes also from the very bright radio core, which has a luminosity comparable to that of the Seyfert galaxy NGC 4151, and the distorted optical structure. An interesting optical feature in the long exposure photograph of NGC 3079 (Fig. 10) is the faint wisp on the east side of the galaxy, near the position of the optical centroid. It clearly extends beyond the projected optical disk and lies on the line through the nucleus and the eastern radio extension. Optical spectroscopic observations are in progress to determine whether this wisp is due to the gas that we postulate to be ejected from the nucleus and responsible for the radio extensions.

The origin of the radio complex in the central region of NGC 4631 remains uncertain as long as the position of the optical nucleus and the orientation of the radio source (elongated or axially symmetric) remain unknown. Far infra-red observations may help to settle the former question. In any case, the short radiative lifetime of the electrons in the central radio source, a factor of 10–100 shorter than the electrons in the surrounding disk, requires that rapid and abundant particle production takes place. All mechanisms discussed for the other three galaxies: particle injection from the nucleus, in-situ acceleration (both requiring gas expulsion as well) and non-linear effects, are possible.

8. Concluding Remarks

8.1. Rate of Occurrence of Anomalous Radio Structures in Spirals

In this paper we have described observations of four spiral galaxies whose radio brightness distributions deviate in varying degress from those "expected" for normal spiral galaxies. These expectations are based on the radio continuum structure of our own galaxy (e.g. Price, 1974), the observed radio morphologies in a large sample of spiral galaxies (van der Kruit, 1973a–c; and various unpublished Westerbork data) and, admittedly, somewhat on my own prejudiced ideas on what a spiral would look like when in a quiet state. In order to place their peculiar radio morphology in the right perspective we have to know how often they occur in a given sample of galaxies, but such data are not yet available. Taking into account our original selection criteria we estimate that about 1% of all spiral galaxies in an optically complete sample have large (> few kpc) anomalous radio structure with *a large surface brightness* ($\gtrsim$100 times that of the base disk). To deduce from this number the birth rate of such structures we need to know how long they can survive as clearly recognizable features over the background disk emission. As shown in the preceding section the radiative lifetimes of these structures are of the order of 10^7 years or less. This estimate of the lifetime is useful only if the mechanism causing their high surface brightness has worked over a period less than 10^7 years such as would be the case if the relativistic electrons observed in these structures were produced in a discrete explosion in the nucleus. If the relativistic electrons are produced in the disk (in-situ) the structures may be much older. An upper limit to their age of about $5\,10^8$ years is deduced, however, from the argument that large collimated structures of the type observed in NGC 4258 and NGC 3079 will be smeared over the disk by the differential rotation[4] of the galaxy. Taking the age limits of 10^7 and $5\,10^8$ years at face value the observed frequency of 1% implies that all galaxies experience such a phase of anomalous radio morphology every 10^9 to $5\,10^{10}$ years. It is often argued that the more luminous and massive galaxies are more likely to contain, or develop, an active nucleus. It is therefore worth noting that NGC 4258, 2146 and 3079 are bright giant spirals with radii of 23, 26 and 40 kpc and absolute magnitudes $M_{pg} = -20.2$, -20.4 and -20.9, respectively (Holmberg, 1958). All three galaxies also have a large central mass concentration as evidenced by their steep rotation curves in the inner regions (van der Kruit, 1974; Benvenuti et al., 1975; d'Odorico, private communication). Thus if only the (say) 10% brightest spirals are able to develop active nuclei and anomalous radio structures, then the frequency of the latter is once every 10^8 to $5\,10^9$ years, i.e., each bright spiral will have gone through several such phases in its lifetime.

The frequency of 1% estimated earlier is about the same as the percentage of Seyfert galaxies among spiral galaxies (Woltjer, 1959; Huchra and Sargent, 1973). This suggests that we are witnessing different evolutionary stages of energetic nuclear activity in spiral galaxies. The available optical and radio data on Seyfert galaxies then suggest that the Seyfert phase must *precede* the phase of anomalous radio morphology.

[4] Note that both NGC 4258 and NGC 3079 have essentially flat rotation curves at radii greater than a few kpc (van Albada and Shane, 1975; Baranne et al., 1974)

8.2. *Manifestation of Nuclear Activity in Spirals Versus Ellipticals*

Although the radio structures of the galaxies discussed in this paper bear a superficial resemblance to those associated with elliptical galaxies, i.e., their two-fold symmetry and their collimation, there are still significant differences. The nonthermal energy content is many orders of magnitudes smaller in the spiral structures and, more significantly, the radio structures in spirals apparently remain confined to a region smaller than or comparable to the optical dimensions. There are some selection effects influencing this comparison, however, the difference will not disappear if proper optical samples are used.

A possible clue to the nature of the radio structures in these spirals may lie in the fact that their radio emission seems to be confined to the equatorial plane. On the assumption that the radio structures are all due to nuclear activity, a conclusion difficult to escape in our opinion, we are then led to the corollary that the energy liberation from the nucleus is collimated perpendicular to the rotation axis and/or that the interstellar medium plays a crucial role in forming, shaping and maintaining the observed radio structures. The first option places a powerful constraint on theories of nuclear activity in spiral galaxies while the second option suggests that there may be other mechanisms (than the currently favored supernovae and galactic nuclei) for accelerating relativistic particles.

Acknowledgements. I am grateful to Prof. J. H. Oort and Prof. H. van der Laan for their role in initiating this (thesis) investigation and for their interest and encouragement throughout its long course. I thank them and Dr. W. W. Shane for comments on an earlier version of the manuscript and Dr. J. Sulentic for suggestions to improve the English.

Drs. G. de Vaucouleurs, H. C. Arp and S. D'Odorico generously send me photographic illustrations and made unpublished results available. I also thank R. D. Ekers and R. Sancisi for the communication of results in advance of publication and Mr. A. A. Schoenmaker for the accurate measurements of reference star positions. The telescope group in Westerbork and the reduction group, draughtsmen and photographic department of the Sterrewacht Leiden all did an excellent job on the data acquisition, calibration and presentation for which I am very grateful. The Westerbork Synthesis Radio Telescope is operated by the Netherlands Foundation for Radio Astronomy with the financial support of the Netherlands Organization for the Advancement of Pure Research (Z.W.O.).

References

van Albada, G.D., Shane, W.W.: 1975, *Astron. Astrophys.* **42**, 433
Alloin, D., Benvenuti, P., D'Odorico, S.: 1975, communication presented at the third European Astronomical Meeting, Tblisi, USSR
Baars, J.W.M., Hooghoudt, B.G.: 1974, *Astron. Astrophys.* **31**, 323
Baldwin, J.E., Pooley, G.G.: 1973, *Monthly Notices Roy. Astron. Soc.* **161**, 127
Baranne, A., Carozzi, N., Comte, G., Courtès, G., Deharveng, J.M., Duflot, R., Monnet, G., Pellet, A.: 1974, Proceedings of the ESO/SRC/CERN conference on research programmes for the new large telescopes, ed. A. Reiz, p. 231
Benvenuti, P., Capacciolo, M., D'Odorico, S.: 1975, *Astron. Astrophys.* **41**, 91
Branson, N.: 1967, *Monthly Notices Roy. Astron. Soc.* **135**, 149
de Bruyn, A.G.: 1976: Ph. D. Thesis, Leiden University
de Bruyn, A.G.: 1977: Astron. Astrophys. **54**, 491
Burbidge, E.M., Burbidge, G.R., Prendergast, K.H.: 1959, *Astrophys. J.* **130**, 739
Burbidge, E.M., Burbidge, G.R., Prendergast, K.H.: 1963, *Astrophys. J.* **138**, 375
Burn, B.J.: 1966, *Monthly Notices Roy. Astron. Soc.* **133**, 67
Casse, J.L., Muller, C.A.: 1974, *Astron. Astrophys.* **31**, 333
Cheriguène, M.F.: 1975, in *Les Dynamique des Galaxies Spirales*, p. 439, Bures-sur-Yvette, ed. L. Weliachew
Cowski, R., Mitteldorf, J.: 1974, *Astrophys. J.* **189**, 51
Crillon, R., Monnet, G.: 1969, *Astron. Astrophys.* **2**, 1
Danver, C.G.: 1942, *Ann. Obs. Lund* No. 10
Ekers, R.D., Sancisi, R.: 1976 (in preparation)
Ginzburg, V.L.: 1974, *Phil. Trans. Roy. Soc. London* A**277**, 463
Gouguenheim, L.: 1969, *Astron. Astrophys.* **3**, 281
Gull, S.F.: 1973, *Monthly Notices Roy. Astron. Soc.* **161**, 47
Gower, J.F.R., Scott, P.F., Wills, D.: 1967, *Mem. Roy. Astron. Soc.* **71**, 49
Harten, R.H.: 1976 (in preparation)
Haynes, M., Sramek, R.A.: 1975, *Astron. J.* **80**, 673
Heeschen, D.S., Wade, C.M.: 1964, *Astron. J.* **69**, 277
Högbom, J.A.: 1974, *Astron. Astrophys. Suppl.* **15**, 417
Högbom, J.A., Brouw, W.N.: 1974, *Astron. Astrophys.* **33**, 289
Holmberg, E.: 1958, *Medd. Lunds Astron. Obs. Ser.* 2, No. 136
Huchra, J.P.: 1976, Ph. D. Thesis, California Institute of Technology, Pasadena
Huchra, J.P., Sargent, W.L.W.: 1973, *Astrophys. J.* **186**, 433
Israel, F.P., Goss, W.M., Allen, R.J.: 1975, *Astron. Astrophys.* **40**, 421
de Jong, M.L.: 1966, *Astrophys. J.* **144**, 553
de Jong, M.L.: 1967, *Astrophys. J.* **150**, 1
Kazès, I., Le Squéren, A.M., Nguyen-Quang-Rieu: 1970, *Astrophys. Letters* **6**, 193
van der Kruit, P.C.: 1973a, *Astron. Astrophys.* **29**, 231
van der Kruit, P.C.: 1973b, *Astron. Astrophys.* **29**, 249
van der Kruit, P.C.: 1973c, *Astron. Astrophys.* **29**, 263
van der Kruit, P.C., Oort, J.H., Mathewson, D.S.: 1972, *Astron. Astrophys.* **21**, 169
van der Kruit, P.C., Allen, R.J.: 1976, *Ann. Review Astron. Astrophys.* **14**, 417
Kulsrud, R.M., Pearce, W.P.: 1969, *Astrophys. J.* **156**, 445
van der Laan, H., Perola, G.C.: 1969, *Astron. Astrophys.* **3**, 468
Lequeux, J.: 1971, *Astron. Astrophys.* **15**, 30
Le Squéren, A.M., Crovisier, J.: 1974, *Astron. Astrophys.* **31**, 447
Maslowski, J.: 1972, *Acta Astron.* **22**, 3
McCutcheon, W.H.: 1973, *Astron. J.* **78**, 18
Miley, G.K.: 1975, Proceedings of the summerschool on the physics of nonthermal radio sources, Urbino, Italy
Pease, F.G.: 1920, *Astrophys. J.* **51**, 276
Pooley, G.G.: 1969, *Monthly Notices Roy. Astron. Soc.* **144**, 143
Price, R.M.: 1974, *Astron. Astrophys.* **33**, 33
Roberts, M.S.: 1968, *Astrophys. J.* **151**, 117
Ruiter, H.R., Arp, H.C., Willis, A.G.: 1976 (in preparation)
Sandage, A.: 1961, The Hubble Atlas of Galaxies, Carnegy Institution of Washington, Washington D. C.
Sandage, A., Tammann, G.A.: 1974, *Astrophys. J.* **194**, 559
Scott, P.F., Shakeshaft, J.R.: 1971, *Monthly Notices Roy. Astron. Soc.* **154**, 19P
Skilling, J.: 1970, *Monthly Notices Roy. Astron. Soc.* **147**, 1
van Someren-Gréve, H.W.: 1974, *Astron. Astrophys. Suppl.* **15**, 343
Sramek, R.A.: 1975, *Astron. J.* **80**, 771
de Vaucouleurs, G.: 1950, *Ann. Astrophys.* **13**, 362
de Vaucouleurs, G., de Vaucouleurs, A.: 1963, *Astrophys. J.* **137**, 363
Véron, M.P., Véron, P., Witzel, A.: 1974, *Astron. Astrophys. Suppl.* **13**, 1
Wardle, J.F.C., Sramek, R.A.: 1974, *Astrophys. J.* **189**, 399
Weiler, K.W.: 1973, *Astron. Astrophys.* **26**, 403
Wentzel, D.G.: 1963, *Astrophys. J.* **137**, 135
Woltjer, L.: 1959, *Astrophys. J.* **130**, 38